Springer

KSME

Journal of Mechanical Science and Technology 29 (8) (2015) 3141~3151
www.springerlink.com/content/1738-494x(Print)/1976-3824(Online)
DOI 10.1007/s12206-015-0713-x

Mathematical modeling of reciprocating pump †

Jong Kyeom Lee, Jun Ki Jung, Jang-Bom Chai and Jin Woo Lee*

Division of Mechanical Engineering, Ajou University, 206 World cup-ro, Suwon-si, 443-749, Korea

(Manuscript Received October 30, 2014; Revised March 20, 2015; Accepted April 6, 2015)

Abstract

A new mathematical model is presented for the analysis and diagnosis of a high-pressure reciprocating pump system with three cylinders. The kinematic and hydrodynamic behaviors of the pump system are represented by the piston displacements, volume flow rates and pressures in its components, which are expressed as functions of the crankshaft angle. The flow interaction among the three cylinders, which was overlooked in the previous models, is considered in this model and its effect on the cylinder pressure profiles is investigated. The tuning parameters in the mathematical model are selected, and their values are adjusted to match the simulated and measured cylinder pressure profiles in each cylinder in a normal state. The damage parameter is selected in an abnormal state, and its value is adjusted to match the simulated and measured pressure profiles under the condition of leakage in a valve. The value of the damage parameter over 300 cycles is calculated, and its probability density function is obtained for diagnosis and prognosis on the basis of the probabilistic feature of valve leakage.

Keywords: Reciprocating pump; Mathematical model; Diagnosis; Valve leakage; Damage parameter; Probability density function

1. Introduction

Reciprocating pumps have been widely used as fluid power pumps in nuclear power plants and hydraulic drive systems of ships and boiler plants. In general, a reciprocating pump system consists of a few cylinders, an outlet manifold, and an accumulator, and the piston in each cylinder is connected to the crankshaft via connecting rods. While the crankshaft is rotating at low speeds, the low-pressure fluid flowing into each cylinder is compressed and discharged through a discharge port when the pressure in the cylinder is greater than that in the outlet manifold. The discharge valves in the cylinders are opened in order, and the opening times of the discharge valves overlap. An abrupt increase in the volume flow rate that occurs when two discharge valves are opened simultaneously is regulated by the accumulator. Therefore, a mathematical-model-based analysis is required to accurately predict the mechanical behavior of each component in the pump design stage and diagnose damage during operation [1-3]. This kind of approach has been applied to not only the reciprocating pump system but also various fluid machines such as compressors and centrifugal pumps [4-6].

A large pressure variation and repetitive contact of active components in the reciprocating pump result in damage to the active and passive mechanical components, which reduce its remaining useful lifetime [7]. Cavitation bubbles can occur in several regions of the pump system owing to an extreme change in the local static pressure [8]. The collapse of these bubbles can result in the application of an impulse-like external force to the mechanical components. The high-speed contact of a valve with a valve stopper generates a repetitive contact force, which could result in cracks around the valve port or the edge of the valve. Therefore, it is crucial to evaluate the existing state of the reciprocating pump from measured physical quantities. A recently proposed condition-based maintenance method requires an improved mathematical model for accurate diagnosis and prognosis [9].

Several researchers have proposed theoretical and numerical models for analyzing the normal state of a reciprocating pump. Johnston [10] numerically modeled a reciprocating pump system with self-acting valves and compared his numerical results with measurement results. Singh and Madavan [11] presented a computer model for the analysis and simulation of a reciprocating pump installation, and their model included the effect of cavitation. Shu et al. [8] employed the Galerkin finite element method for developing a distributed parameter model of pipeline transmission line behavior. Henshaw [12] developed a valve dynamics model for calculating pressure drops in a valve assembly. Able [13] further explained the acceleration head phenomena by modeling the pump and the suction system as a damped, forced vibration system. Shcherba et al. [14] analyzed the impact of major design and operational parameters on the efficiency and per-

*Corresponding author. Tel.: +82 31 219 3659, Fax.: +82 31 219 1611
E-mail address: jinwoolee@ajou.ac.kr
† Recommended by Editor Yeon June Kang

formance of a reciprocating pump. Rudolf et al. [15] determined optimum parameters for maintaining flow at minimum reservoir pressure through modeling and experimental data. These research results certainly contributed to model-based theoretical approaches for identifying the parameters of normally operating systems. However, these models considered only one cylinder or ignored the flow interaction between more than two cylinders, and it is difficult to apply them to system diagnosis problems because they do not describe an abnormal state of a reciprocating pump system.

The flow interaction between cylinders whose discharge valves are simultaneously open should be considered in an analytical model of a reciprocating pump system. For a three-cylinder reciprocating pump, one end of each connecting rod whose other end is connected to the associated piston is connected to the same crankshaft. In a normal operating condition, the crank angles when each cylinder starts to open its discharge valve differ by 120°, and the outgoing flow from each cylinder merges in the outlet manifold. Since the open duration angle of each discharge valve is more than 150°, the opening times of two discharge valves are always overlapping. When two discharge valves are open, the flow interaction between two associated cylinders could affect the pressure in the outlet manifold, which in turn would change the pressure of the outgoing flow of the reciprocating pump system.

A mathematical model used in model-based diagnosis methods should well describe not only the normal state but also the abnormal state of the actual system. In the normal state, normal state parameters in the model developed under ideal assumptions are tuned by comparing the measured and simulated results. In the abnormal state, damage parameters should be defined to determine whether damage has occurred and to represent the degree of the damage. We calculated a damage parameter, which is defined for valve leakage, over 300 cycles and obtained its probability density function for diagnosis and prognosis on the basis of the probabilistic feature of valve leakage.

This paper is organized as follows. A new mathematical model of a reciprocating pump system is developed using kinematics, hydrodynamics, and thermodynamics. The model considers the flow interaction in the outlet manifold and the effect of valve leakage. Then the tuning parameters and damage parameter in the mathematical model are selected for identifying the normal and abnormal states. The specific values of the tuning parameters and the probabilistic distribution of the damage parameter are obtained by comparing experimental and simulated results.

2. Mathematical modeling

Fig. 1(a) shows the schematic diagram of the flow loop manufactured in this work, wherein the reciprocating pump system shown in Fig. 1(b) consists of three identical cylinders, one outlet manifold, and one accumulator, as shown in Fig. 1(c). Each cylinder has one suction valve, one discharge valve,

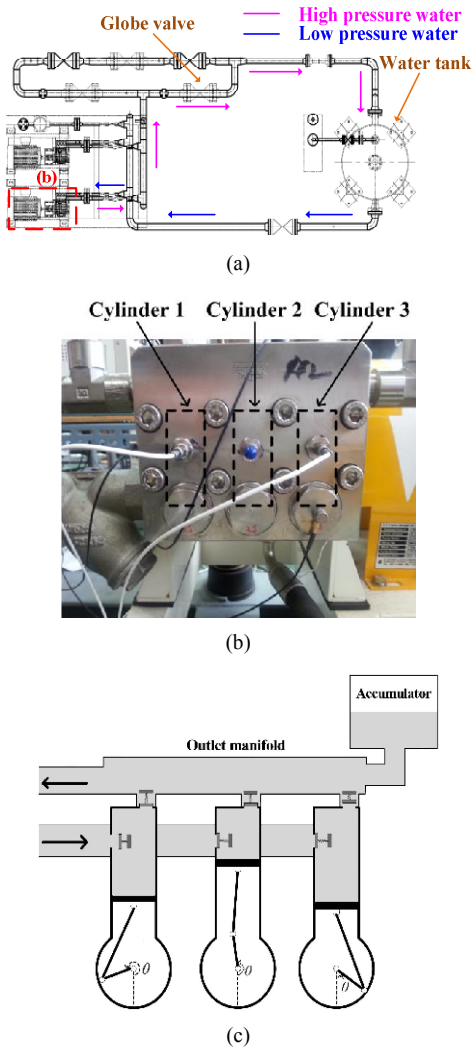

Fig. 1. Reciprocating pump system: (a) Schematic diagram of flow loop manufactured in this work; (b) reciprocating pump with three cylinders; (c) schematic diagram of reciprocating pump.

and one piston, as shown in Fig. 2(a). In an actual system, each piston is connected to the same crankshaft, even though each crankshaft is illustrated separately in the schematic diagram in Fig. 1(c). The suction valve is open or closed depending on the pressure difference between the cylinder and the suction pipe, and the discharge valve is open or closed depending on the pressure difference between the cylinder and the outlet.

Several reasonable assumptions are made for developing a simplified mathematical model, as follows. The operating fluid is an incompressible fluid, e.g., water. The crankshaft rotates at a constant speed. The suction valve is closed at the Bottom dead center (BDC), and the discharge valve is closed at the Top dead center (TDC). Two valves open only by the pressure difference between two sides of one valve and the valve spring force. Under these assumptions, a mathematical model is first developed for a single cylinder reciprocating pump in the normal state and then extended for three-cylinder

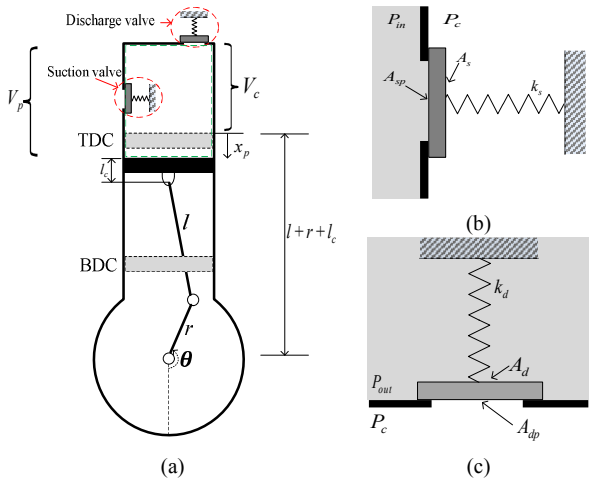

Fig. 2. Single cylinder reciprocating pump: (a) Schematic diagram; (b) suction valve; (c) discharge valve.

models with the outlet manifold and accumulator. Then, the abnormal state of valve leakage is considered in the model.

2.1 Normal operating state

2.1.1 Modeling of single cylinder reciprocating pump

As shown in Fig. 2(a), the piston in a single cylinder reciprocating pump moves up and down between the BDC and the TDC while the crankshaft is constantly rotating. The volume flow rate (Q_c) of the cylinder as expressed in Eq. (1) is developed using the Reynolds transport theorem [16]:

$$Q_c = Q_p - Q_s + Q_d \,, \tag{1}$$

where Q_p is the volume flow rate attributed to piston displacement, Q_s is the volume flow rate of the fluid flowing in through the suction port, and Q_d is the volume flow rate of the fluid flowing out through the discharge port. All the volume flow rates are functions of the rotation angle θ of the crankshaft, and Q_p is defined as in Eq. (2):

$$Q_p = \frac{dV_p}{dt} \,, \tag{2a}$$

$$V_p = A_p x_p + V_c \,, \tag{2b}$$

$$x_p = r\left(1+\cos\theta\right) + l\left(1-\sqrt{1-r^2/l^2\times\sin^2\theta}\right), \tag{2c}$$

where V_p is the cylinder volume changing with the piston displacement x_p, which is a function of the connecting rods (r and l in Eq. (2c)) and the rotation angle θ of the crankshaft [17]. Further, A_p and V_c denote the cross-sectional area of the piston and the clearance volume, respectively. The volume flow rates through the valve port (Q_s and Q_d) are expressed as Eqs. (3) and (4), respectively [18]:

$$Q_s = A_{sp} C_{in} \sqrt{2\left(P_{in} - P_c\right)/\rho} \,, \tag{3}$$

$$Q_d = A_{dp} C_{out} \sqrt{2\left(P_c - P_{out}\right)/\rho} \,, \tag{4}$$

where A_{sp} and A_{dp} are the cross-sectional areas of the suction and discharge ports, respectively, and C_{in} and C_{out} are flow coefficients. The variables P_{in} and P_{out} denote pressures in the suction pipe and the outlet, respectively. Further, P_c and ρ denote the pressure in the cylinder and the fluid density, respectively.

Consider the elastic bulk modulus β in Eq. (5), which correlates the volume and pressure inside the cylinder changing with the rotation angle of the crankshaft:

$$\beta = -V_p \frac{dP_c}{dV_p} \,, \tag{5}$$

which is converted by using the angular speed ω of the crankshaft to Eq. (6):

$$\frac{dP_c}{d\theta} = -\frac{\beta}{\omega}\frac{Q_c}{V_p} \,. \tag{6}$$

The opening angles of the suction and discharge valves are determined by the force difference between two sides of each valve. Just before each valve starts to open as shown in Figs. 2(b) and 2(c), the cross-sectional areas to which pressures on both sides are applied should be determined carefully. The variables A_s and A_d denote the cross-sectional areas of the suction and discharge valves, respectively. The vertical cross-section of the actual valve in Fig. 3(a) is illustrated in Fig. 3(b). Since the surfaces of the two sides of the actual valve are not flat while the pressure is applied normally to the valve surface, the multiplication of the pressure and the horizontal cross-sectional area of the surface is not equal to the net force resulting from the associated pressure. Therefore, the additional force (ΔF_s or ΔF_d) should be considered in the free body diagram for each valve as shown in Figs. 3(c) and 3(d), where x_s and x_d denote the displacements of the suction and discharge valves, respectively [19]. The initial compression of suction and discharge valve springs with spring constants k_s and k_d is denoted by x_s^{ini} and x_d^{ini}, respectively. While the suction valve is open when P_c satisfies Eq. (7a), the discharge valve is open when P_c satisfies Eq. (7b). The opening angles (θ_3 and θ_1) of the suction and discharge valves in Eqs. (8a) and (8b) are determined by the equality conditions in Eqs. (7a) and (7b), respectively.

$$P_{in}A_{sp} \geq P_c A_s + \Delta F_s + k_s x_s^{ini} \,, \tag{7a}$$

$$P_c A_{dp} \geq P_{out} A_d + \Delta F_d + k_s x_d^{ini} \,, \tag{7b}$$

At $\theta = \theta_3$,

$$P_c = \frac{\varepsilon_s A_{sp}}{A_s} P_{in} - \frac{k_s x_s^{ini}}{A_s}, \quad \varepsilon_s = 1 - \frac{\Delta F_s}{A_{sp}}\frac{1}{P_{in}} \tag{8a}$$

At $\theta = \theta_1$,

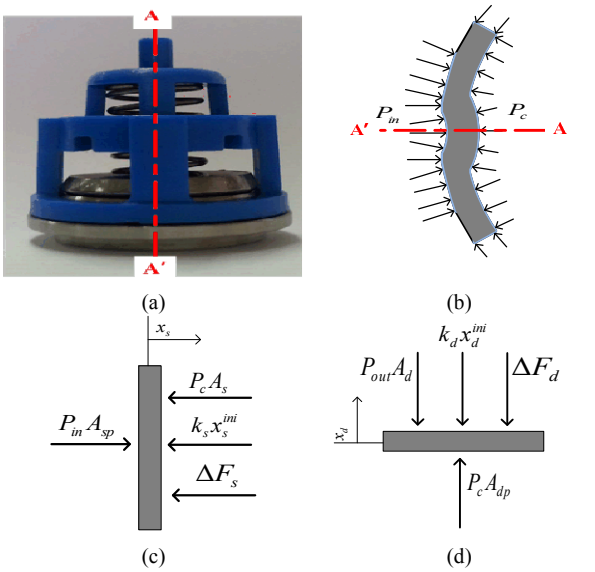

Fig. 3. Valve used in suction and discharge ports: (a) Actual valve; (b) vertical cross-section of valve; (c) free body diagram for suction valve; (d) free body diagram for discharge valve.

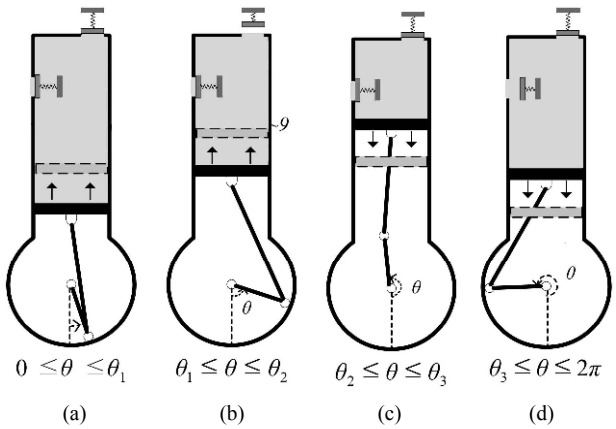

Fig. 4. Operating modes of one cylinder in reciprocating pump: (a) Compression mode; (b) discharge mode; (c) expansion mode; (d) suction mode.

$$P_c = \frac{\varepsilon_d A_d}{A_{dp}} P_{out} + \frac{k_d x_d^{ini}}{A_{dp}}, \quad \varepsilon_d = 1 + \frac{\Delta F_d}{A_d} \frac{1}{P_{out}}, \tag{8b}$$

where ε_s and ε_d are the correction factors of the cross-sectional areas.

The kinematic and thermodynamic behaviors of a reciprocating pump system are divided into four operating modes depending on the opening and closing of the discharge and suction valves and the piston displacement, as shown in Fig. 4: (a) compression mode, (b) discharge mode, (c) expansion mode, and (d) suction mode. Therefore, the volume flow rate of the cylinder in each mode is specified differently depending on the operating mode, as expressed in Eq. (9):

Compression mode: $Q_c = Q_p$, (9a)

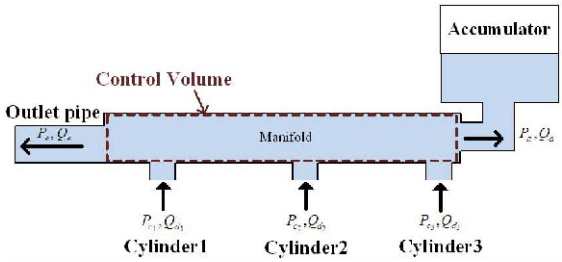

Fig. 5. Analysis model of outlet manifold with accumulator connected to three cylinders and outlet pipe.

Discharge mode: $Q_c = Q_p + Q_d$, (9b)

Expansion mode: $Q_c = Q_p$, (9c)

Suction mode: $Q_c = Q_p - Q_s$. (9d)

2.1.2 Modeling of outlet manifold

As shown in Fig. 5, the outgoing flow of each cylinder merges in the outlet manifold with the accumulator, and the high-pressure fluid in the outlet manifold flows into the outlet pipe. To develop a mathematical model for the outlet manifold, the control volume is defined and represented by the brown dotted line as shown in Fig. 5. Eq. (10) is obtained by considering the mass conservation law for the control volume and assuming that the density of fluid is constant [18]:

$$Q_{in} - Q_{out} = 0, \tag{10a}$$

$$Q_{in} = Q_{d_1} + Q_{d_2} + Q_{d_3}, \tag{10b}$$

$$Q_{out} = Q_e + Q_a, \tag{10c}$$

where the volume flow rate of the fluid flowing into the manifold, Q_{in}, is the sum of the volume flow rates of the fluids flowing out from each cylinder ($Q_{d,1}, Q_{d,2}, Q_{d,3}$); and the volume flow rate of the fluid flowing out from the outlet manifold, Q_{out}, consists of the volume flow rates (Q_e and Q_a) of the fluid flowing into the outlet pipe and accumulator.

Eq. (11a) is obtained by considering the mechanical energy balance for the control volume and by assuming that the temperature change and the height difference are ignored [18]:

$$\dot{E}_m - \dot{E}_e - \dot{E}_a = 0, \tag{11a}$$

$$\dot{E}_e = \rho Q_e \left(\frac{P_e}{\rho} + \frac{1}{2} \left(\frac{Q_e}{A_e} \right)^2 \right) \tag{11b}$$

$$\dot{E}_a = \rho Q_a \left(\frac{P_a}{\rho} + \frac{1}{2} \left(\frac{Q_a}{A_a} \right)^2 \right)$$

$$\dot{E}_m = \sum_{i=1}^{3} \rho Q_{d,i} \left(\frac{P_{c,i}}{\rho} + \frac{1}{2} \left(\frac{Q_{d,i}}{A_d} \right)^2 \right), \tag{11c}$$

$$\dot{E}_m = \rho Q_m \left(\frac{P_m}{\rho} + \frac{1}{2} \left(\frac{Q_m}{A_m} \right)^2 \right), \tag{11d}$$

where $\dot{E}_e$ and $\dot{E}_a$ denote the mechanical powers of the fluids flowing into the outlet pipe and accumulator, respectively. The total mechanical power $\dot{E}_m$ of the fluids flowing into the outlet manifold in Eq. (11c) is expressed as the functions $P_{c,i}$ and $Q_{d,i}$ which denote the pressure inside cylinder i (i = *1,2,3*) and the volume flow rate of the fluid flowing out from cylinder i, respectively. Furthermore, the equivalent pressure P_m and equivalent volume flow rate Q_m of fluid flowing into the outlet manifold are defined as in Eq. (11d).

The accumulator used to regulate the volume flow rate of the outlet manifold is filled with nitrogen gas and liquid. The pressure P_a and volume flow rate Q_a of the liquid in the accumulator are related as in Eq. (12), where P_n and V_n are the pressure and volume, respectively, of the nitrogen gas [13]:

$$Q_a = \frac{V_n}{P_n}\frac{dP_a}{d\theta}\omega \,. \tag{12}$$

The pressure P_e and volume flow rate Q_e of the fluid flowing in the outlet pipe of cross-sectional area A_e from the outlet manifold are related as in Eq. (13), where Z_e is the flow resistance due to the cross-sectional shape of the outlet pipe and friction [12]:

$$P_e = Z_e Q_e \,. \tag{13}$$

2.2 Abnormal operating state

The abnormal operating state considered in this work is assumed to be attributed to valve leakage. In the normal state, the fluid flows into the cylinder from the inlet pipe only during the suction mode and flows out from the cylinder to the outlet manifold only during the discharge mode. However, when there is a leakage in the discharge/suction valve, the flow between the inlet pipe and the cylinder or between the cylinder and the outlet manifold occurs even during the other operating modes. The volume flow rate Q_l attributed to the leakage is expressed as in Eq. (14):

$$Q_l = \begin{cases} Q_{ld} & \text{for suction valve leakage} \\ Q_{ld} & \text{for discharge valve leakage} \end{cases}, \tag{14a}$$

$$Q_{ls} = A_{ls}C_{in}\sqrt{2\left|P_{in}-P_c\right|/\rho}\cdot\left(P_{in}\text{-}P_c\right)/\left|P_{in}-P_c\right|, \tag{14b}$$

$$Q_{ld} = A_{ld}C_{in}\sqrt{2\left|P_c-P_{out}\right|/\rho}\cdot\left(P_c\text{-}P_{out}\right)/\left|P_c-P_{out}\right|, \tag{14c}$$

where A_{ls} and A_{ld} are the effective cross-sectional areas related to the valve leakage. The volume flow rate Q_c of the cylinder in Eq. (9) is replaced with that expressed in Eqs. (15) and (16) in the abnormal state under consideration.

In case of suction valve leakage

Compression mode: $Q_c = Q_p - Q_{ls}$, (15a)

Discharge mode: $Q_c = Q_p + Q_d - Q_{ls}$, (15b)

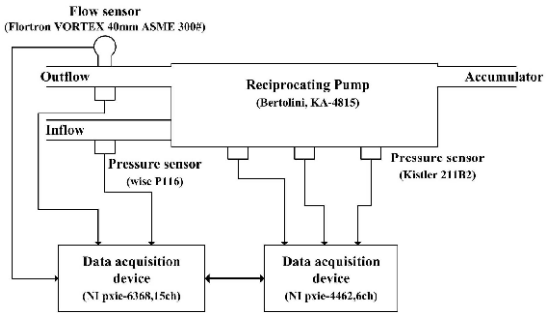

(a)

(b)

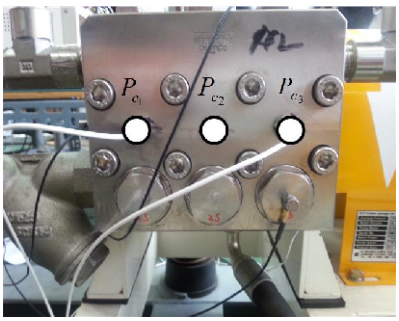

(c)

Fig. 6. Experiment for measuring pressures in reciprocating pump system: (a) Experimental setup; (b) actual reciprocating pump used in this work; (c) locations of pressure sensors.

Expansion mode: $Q_c = Q_p - Q_{ls}$, (15c)

Suction mode: $Q_c = Q_p - Q_s$. (15d)

In case of discharge valve leakage

Compression mode: $Q_c = Q_p + Q_{ld}$, (16a)

Discharge mode: $Q_c = Q_p + Q_d$, (16b)

Expansion mode: $Q_c = Q_p + Q_{ld}$, (16c)

Suction mode: $Q_c = Q_p - Q_s + Q_{ld}$. (16d)

3. Probabilistic estimation of damage parameters

3.1 Experiment

Fig. 6(a) shows the schematic diagram of the experimental setup. Five pressure sensors (Kistler 211B2 and Wise P116) were used to measure the pressures of the reciprocating pump system used in the experiment (KA-4815, Bertolini), as shown

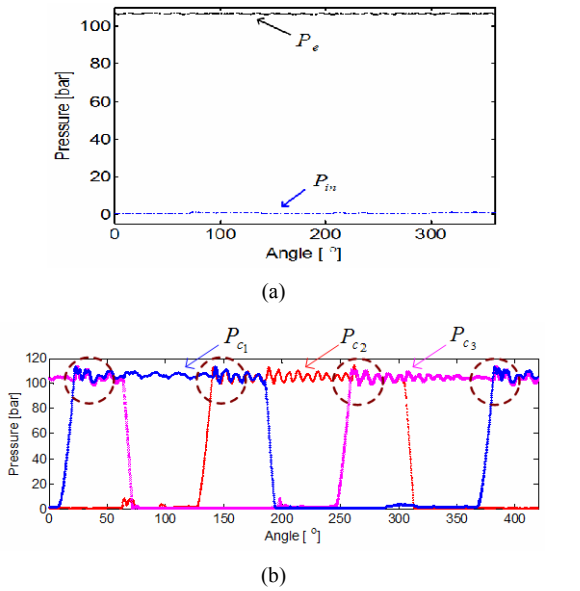

Fig. 7. Measured pressures: (a) Inlet pipe and outlet pipe; (b) three cylinders.

in Fig. 6(b). Two pressure sensors measured the pressures (P_{in} and P_e) of the inlet and outlet pipes of the reciprocating pump system, and the remaining three pressure sensors measured the pressure ($P_{c,i}$) inside each cylinder, as shown in Fig. 6(c). A flow rate sensor (Flowtron VORTEX) was installed in the outlet pipe to measure the volume flow rate of the outgoing flow. The experiment was performed over 300 cycles.

The measured pressure profiles well represented the flow interaction and damage effect. Fig. 7(a) shows the measured pressure profiles of the inlet and outlet pipes during one cycle in the normal state, and Fig. 7(b) shows the simultaneously measured pressure profiles of the three cylinders. Whenever the discharge valve of one cylinder started to open, pressure fluctuation was observed in one of the other two pressure profiles owing to flow interaction between two cylinders (see the brown dotted circles in Fig. 7(b)). Fig. 8 shows a comparison of the pressure profiles of the three cylinders in the normal and abnormal states. The abnormal state was implemented by intentionally wearing the suction valve of cylinder 1, whose pressure is denoted by P_{c1} in Fig. 6(a). This comparison reveals that only cylinder 1 underwent wear of the suction valve. Owing to the suction valve leakage, the discharge valve started to open later in comparison to its opening in the normal state. It was difficult to observe a noticeable difference between the pressure profiles in the normal and abnormal states in the other two cylinders.

3.2 Simulation

Tuning parameters were selected for improving the accuracy of the developed mathematical model in the normal state, and the damage parameter was established for describing the degree of damage in the abnormal state. The parameters of the

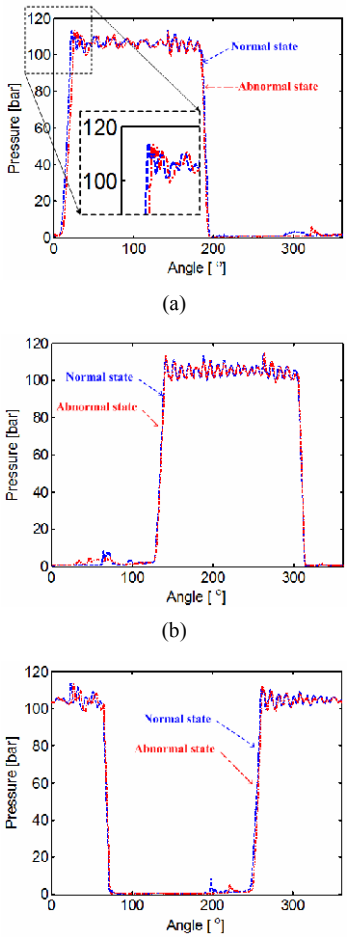

Fig. 8. Comparison of pressure profiles in normal and abnormal states in the case of damage at suction valve of cylinder 1: (a) Cylinder 1; (b) cylinder 2; (c) cylinder 3.

mathematical model in the normal state were classified as either fixed parameters or tuning parameters. Fixed parameters are the intrinsic parameters of the mechanical system under consideration, such as the lengths of connecting rods and the cross-sectional area of the piston. Tuning parameters, on the other hand, are adjusted to match the simulated behavior of the mathematical model to the measured behavior of the actual system. The values of the fixed parameters are listed in Table 1. The specific values of the tuning parameters were determined by comparing the calculated and measured pressures of the three cylinders in the normal state. The damage parameter describes the degree of valve wear, which results in valve leakage. Its specific value was also determined by comparing the calculated and measured pressures of the three cylinders in the abnormal state.

The pressure inside each cylinder was calculated by considering the opening and closing of the suction and discharge valves of each cylinder and the flow interaction between the cylinders. On the basis of detailed investigations of the measured pressure profiles for the three cylinders, the operating mode of the reciprocating pump system was divided into 12

Table 1. Values of fixed parameters in mathematical model of reciprocating pump.

Symbol	Parameter	Value
A_a (m^2)	Cross-sectional area of accumulator pipe	2×10^{-3}
A_d (m^2)	Cross-sectional area of discharge valve	3.94×10^{-4}
A_{dp} (m^2)	Cross-sectional area of discharge port	2.14×10^{-4}
A_e (m^2)	Cross-sectional area of outlet pipe	2×10^{-3}
A_p (m^2)	Cross-sectional area of piston	4.91×10^{-4}
A_s (m^2)	Cross-sectional area of suction valve	3.94×10^{-4}
A_{sp} (m^2)	Cross-sectional area of suction port	2.14×10^{-4}
k_s (N/m)	Spring constant of suction valve	420
k_d (N/m)	Spring constant of discharge valve	420
l (m)	Length of longer connecting rod	0.48
r (m)	Length of shorter connecting rod	0.12
P_n (bar)	Pressure of nitrogen gas in accumulator	100
V_n (m^3)	Clearance volume	1.45×10^{-4}
x_d^{ini} (m)	Initial compression of discharge valve spring	0.001
x_s^{ini} (m)	Initial compression of suction valve spring	0.001
Z_e (kg/m^{4}s)	Flow resistance at outlet	1.57×10^{10}
ρ (kg/m^3)	Fluid density	1000
ω (rad/s)	Angular velocity of crankshaft	122.5

Table 2. Operating modes of reciprocating pump system with three cylinders.

Mode	Cylinder 1	Cylinder 2	Cylinder 3
1	Compression	Suction	Discharge
2	Discharge	Suction	Discharge
3	Discharge	Suction	Expansion
4	Discharge	Suction	Suction
5	Discharge	Compression	Suction
6	Discharge	Discharge	Suction
7	Expansion	Discharge	Suction
8	Suction	Discharge	Suction
9	Suction	Discharge	Compression
10	Suction	Discharge	Discharge
11	Suction	Expansion	Discharge
12	Suction	Suction	Discharge

sets of operating modes, as listed in Table 2. In the simulation, the derivative terms with respect to the crankshaft angle in Eqs. (2a), (5), and (12) were calculated with $\Delta\theta$ by using the forward Euler method as expressed in Eq. (17):

$$\frac{dF(\theta)}{d\theta} \cong \frac{F(\theta+\Delta\theta)-F(\theta)}{\Delta\theta}, \tag{17}$$

where $F(\theta)$ denotes the functions of the rotation angle in Eqs. (2a), (5), and (12).

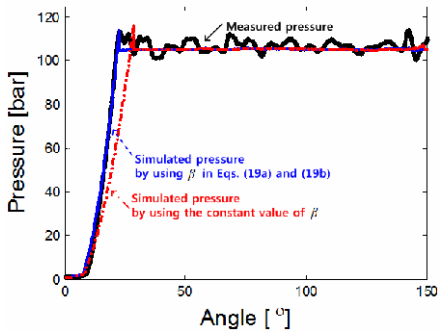

(a)

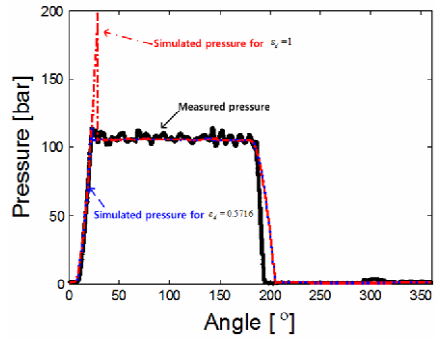

(b)

Fig. 9. Comparison of pressure profiles: (a) β fitting; (b) ε_d fitting.

3.3 Values of tuning and damage parameters

The specific values of the tuning parameters were determined by comparing the measured and simulated pressure profiles inside the cylinders in the normal state, especially the pressure profiles in the compression mode. In the simulation, the measured pressures at the inlet and outlet pipes were used as input data, and the pressure in each cylinder was calculated as output data. The bulk modulus β and correction factor (ε_d) were selected as the tuning parameters because the slope and peak values of the pressure during the compression mode in the normal state depend strongly on β and ε_d, respectively. The linear and quadratic equations in Eq. (18) were used as the fitting equations, which are functions of pressure inside the cylinder:

$$\beta = a_1 P_c \quad \text{for} \quad P_c \le P_{ref}, \tag{18a}$$

$$\beta = a_2 P_c^2 + b_2 P_c + c_2 \quad \text{for} \quad P_c \ge P_{ref}, \tag{18b}$$

where a_1, a_2, b_2, c_2 are the fitting coefficients, and the reference pressure P_{ref} is set to 3 bar. Fig. 9(a) compares the pressure profiles simulated by using Eqs. (18a) and (18b) and by using the constant value of β at 1 bar with the measured result. Fig. 9(b) compares the pressure profiles simulated by using the adjusted value of ε_d and by using $\varepsilon_d = 1$ with the measured result. The peak value of the simulated pressure was matched to the peak value of the measured result by adjusting the value of ε_d. The value of ε_s was adjusted to match the

Table 3. Specific values of tuning parameters of the mathematical model in the normal state.

Symbol	Quantity	Value
ε_d	Correction factor of cross-sectional area of discharge valve	0.5716
ε_s	Correction factor of cross-sectional area of suction valve	1.8
a_1	Coefficient of linear term in Eq. (18a)	1.2×10^{-2}
a_2	Coefficient of quadratic term in Eq. (18b)	6.51×10^{-2}
b_2	Coefficient of linear term in Eq. (18b)	4.47×10
c_2	Coefficient of constant term in Eq. (18b)	2.31×10^{4}

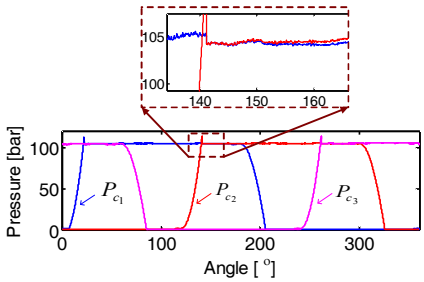

(a)

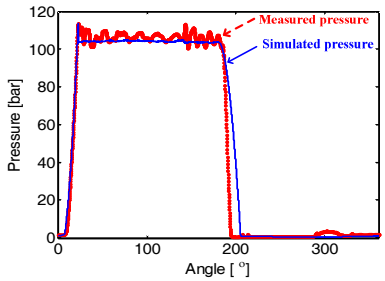

(b)

Fig. 10. Simulation results: (a) Pressure profiles of three cylinders obtained using mathematical model in a normal state; (b) comparison of measured and simulated pressure profiles of cylinder 1 in an abnormal state.

dip values of the simulated and measured pressures during the suction mode. The pressure profiles inside the cylinders calculated using the adjusted values of the tuning parameters listed in Table 3 are shown in Fig. 10(a). The brown rectangle inset represents the flow interaction, which was also observed in the measured results shown in Fig. 7(b). The adjusted values were averaged over 300 cycles.

The specific value of the damage parameter was also determined by comparing the measured and simulated pressure profiles inside the cylinders in the abnormal state. The normal state valve and abnormal state valve are compared in Fig. 11. In this work, we considered two abnormal states depending on the damage degree of the valve as shown in Figs. 11(b) and 11(c). The cross-sectional area A_l (A_{ls} and A_{ld}) in Eq. (14) was taken as the damage parameter in the abnormal state, because it well represents the change in the volume flow rate due to valve leakage. Fig. 10(b) compares the pressure profile inside

Table 4. Specific values of coefficients in Eq. (19) used to represent the probability distribution of damage parameter.

	Damaged valve in Fig. 11(b)		Damaged valve in Fig. 11(c)	
	Damaged suction valve	Damaged discharge valve	Damaged suction valve	Damaged discharge valve
μ	3.3310×10^{-6}	4.9984×10^{-7}	6.7668×10^{-6}	2.0422×10^{-6}
σ	3.0143×10^{-6}	1.1002×10^{-6}	3.5548×10^{-6}	1.5784×10^{-6}

(a) (b) (c)

Fig. 11. Valve photos: (a) normal state; (b) abnormal state I; (c) abnormal state II.

the cylinder, which is calculated by using the adjusted value of the damage parameter and the specific values of the tuning parameters listed in Table 3, with the measured result for one cycle. Since the representative value of the damage parameter does not always indicate the degree of damage, its probability distribution is meaningful for calculating the remaining useful lifetime based on probability [20]. Fig. 12 show the damage parameter versus frequency graphs. Figs. 12(a) and 12(b) show the distribution of the damage parameter value when the damage valve in Fig. 11(b) was used in the suction port or discharge port. Figs. 13(a) and 13(b) show the distribution of the damage parameter value when the damage valve in Fig. 11(c) was used in the suction port or discharge port. The probability density function of the damage parameter resulting from the wear of the suction and discharge valves was obtained by using the curve-fitted equation in Eq. (19) and the distributions in Fig. 12 as shown in Fig. 13.

$$y = \frac{1}{\sigma\sqrt{2\pi}} \cdot \exp\left(-\left(\frac{x-\mu}{2\sigma^2} \right)^2 \right), \tag{19}$$

where y represents the probability density of the damage parameter denoted by x. The specific values of the mean value (μ)and the standard deviation (σ) for four cases in Fig. 12 are compared in Table 4.

The solid and dotted lines in Fig. 13 represent the probability density distribution when the valves in Fig. 11(b) and Fig. 11(c) are used in the suction/discharge port, respectively. As shown in Fig. 11, the damage amount of the valve in Fig. 11(c) is obviously more than that in Fig. 11(b). Figs. 13(a) and 13(b) well represent the damage difference in Figs. 11(b) and 11(c). As compared in Table 4, the mean value of the damage parameter of the suction valve when the valve in Fig. 11(b) is used in the suction port is about twice larger than that when the valve in Fig. 11(c) is used in the suction port. This phe-

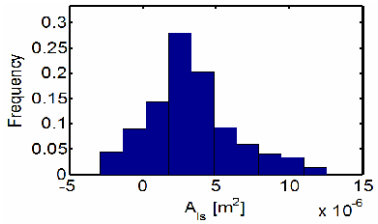

(a)

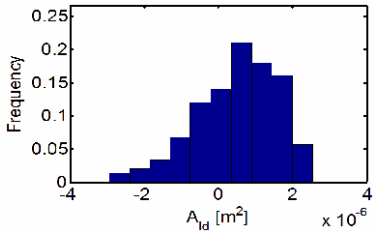

(b)

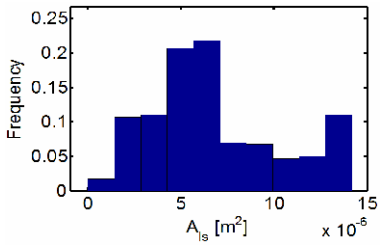

(c)

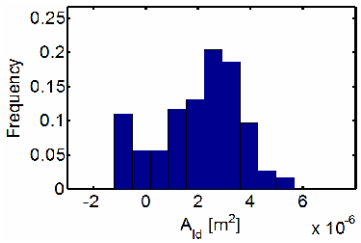

(d)

Fig. 12. Frequency of damage parameter when the damaged valve was used: (a) when the damage valve in Fig. 11(b) was used in the suction port; (b) when the damage valve in Fig. 11(b) was used in the discharge port; (c) when the damage valve in Fig. 11(c) was used in the suction port; (d) when the damage valve in Fig. 11(c) was used in the discharge port.

nomenon is also found for the damaged discharge value as shown in Fig. 13(b). It implies that the current model-based damage estimation method could probabilistically represent the damage degree well as the damage amount increases.

4. Conclusions

A reciprocating pump system with three cylinders was mathematically modeled for predicting the pressure profiles and diagnosing the abnormal state of the system. Since the model was developed under ideal assumptions, the tuning parameters were adjusted to match the simulated pressure profiles inside the cylinders to the measured results in the

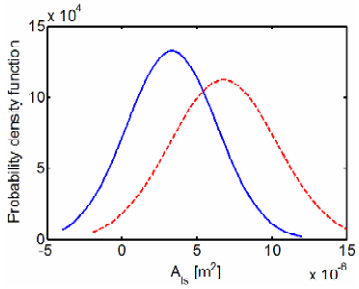

(a)

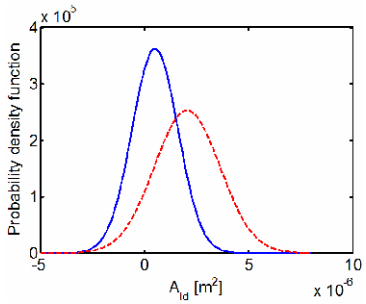

(b)

Fig. 13. Comparison of the probability density function depending on its damage degree when the damaged valve in Fig. 11 was used: (a) when the damage valve in Figs. 11(b) and 11(c) were used in the suction port; (b) when the damage valve in Figs. 11(b) and 11(c) were used in the discharge port.

normal state. The damage parameter was calculated over 300 cycles in the abnormal state, and its probability density functions were obtained for diagnosis and prognosis based on the probabilistic feature of the damage component. Even if the mathematical-model-based-system-identification method was developed in case of valve damage in a reciprocating pump system, it could be extended to obtain the probability density function of any damage parameter, which could strongly affect the remaining useful lifetime in the reciprocating pump system.

Acknowledgment

This work was supported by the International Collaborative Energy Technology R&D Program of the Korea Institute of Energy Technology Evaluation and Planning (KETEP), granted financial resource from the Ministry of Trade, Industry and Energy of the Republic of Korea (No. 20128540010020).

Nomenclature

A_a : Cross-sectional area of accumulator pipe
A_d : Cross-sectional area of discharge valve
A_{dp} : Cross-sectional area of discharge port
A_e : Cross-sectional area of outlet pipe
A_{ld} : Effective cross-sectional area related to discharge valve leakage
A_{ls} : Effective cross-sectional area related to suction valve

leakage
A_m : Equivalent cross-sectional area of outlet manifold
A_p : Cross-sectional are of piston
A_s : Cross-sectional are of suction valve
A_{sp} : Cross-sectional are of suction port
C_{in} : Flow coefficient of fluid flowing into cylinder
C_{out} : Flow coefficient of fluid flowing out of cylinder
$\dot{E}_a$: Mechanical power of fluid flowing into accumulator
$\dot{E}_e$: Mechanical power of fluid flowing into outlet pipe
$\dot{E}_m$: Total mechanical power of fluid flowing into outlet manifold
ΔF_d : Additional force applied to discharge valve
ΔF_s : Additional force applied to suction valve
k_d : Spring constant of discharge valve
k_s : Spring constant of suction valve
l : Length of longer connecting rod
r : Length of shorter connecting rod
P_a : Pressure of liquid in accumulator
P_c : Pressure inside cylinder
$P_{c,i}$: Pressure inside cylinder i (i = 1,2,3)
P_{in} : Pressure in suction pipe
P_m : Equivalent pressure of fluids flowing into outlet manifold
P_n : Pressure of nitrogen gas in accumulator
P_{out} : Pressure in outlet
Q_a : Volume flow rate of liquid in accumulator
Q_c : Volume flow rate of cylinder
Q_d : Volume flow rate of fluid flowing out through discharge port
$Q_{d,i}$: Volume flow rate fluid flowing out of cylinder i (i = 1, 2, 3)
Q_e : Volume flow rate of fluid flowing into outlet pipe
Q_{in} : Volume flow rate of fluid flowing into outlet manifold
Q_l : Volume flow rate attributed to leakage
Q_m : Equivalent volume flow rate of outlet manifold
Q_{out} : Volume flow rate of fluid flowing out from outlet manifold
Q_p : Volume flow rate attributed to piston displacement
V_c : Clearance volume
V_n : Volume of nitrogen gas in accumulator
V_p : Cylinder volume changing with piston displacement
x_d^{ini} : Initial compression of discharge valve spring
x_d : Displacement of discharge valve
x_p : Piston displacement
x_s^{ini} : Initial compression of suction valve spring
x_s : Displacement of suction valve
Z_e : Flow resistance at outlet
β : Elastic bulk modulus
ε_d : Correction factor of cross-sectional area of suction valve
ε_d : Correction factor of cross-sectional area of discharge valve
θ : Rotation angle of crankshaft
θ_1 : Opening angle of discharge valve
θ_2 : Closing angle of discharge valve
θ_3 : Opening angle of suction valve
ρ : Fluid density

References

[1] Y. J. An and B. R. Shin, Numerical investigation of suction vortices behavior in centrifugal pump, *JMST*, 25 (3) (2011) 767-772.

[2] W. Wan and W. Huang, Investigation on complete characteristics and hydraulic transient of centrifugal pump, *JMST*, 25 (10) (2011) 2583-2590.

[3] S. Y. Lee, Acoustic diagnosis of a pump by using neural network, *JMST*, 20 (12) (2006) 2079-2086.

[4] H. M. Chae and C. N. Kim, A numerical study with FSI mode on the characteristics of pressure fluctuation and discharge valve motion in rotary compressors with single and dual muffler, *International J. of Precision Engineering and Manufacturing*, 11 (4) (2010) 589-596.

[5] W. N. Yoon, M. S. Kang, N. K. Jung, J. S. Kim and B. H. Choi, Failure analysis of the defect-induced blade damage of a compressor in the gas turbine of a cogeneration plant, *International J. of Precision Engineering and Manufacturing*, 13 (5) (2012) 717-722.

[6] Y. Arai, A. Inada, J. Yang and W. Gao, A high speed and compact system for profile measurement of scroll compressors, *International J. of Precision Engineering and Manufacturing*, 10 (5) (2010) 27-32.

[7] T. Khan and P. Ramuhalli, A recursive Bayesian estimation method for solving electromagnetic nondestructive evaluation inverse problems, *IEEE Transactions on Magnetics*, 44 (7) (2008) 1845-1855.

[8] J. J. Shu, C. R. Burrow and K. A. Edge, Pressure pulsations in reciprocating pump piping systems-Part 1: modeling, *Proc. of the Institution of Mechanical Engineers, Part 1: J. of Systems and Control Engineering*, 211 (3) (1997) 229-235.

[9] D. Jarell, D. Sisk and L. Bond, Prognostics and condition based maintenance (CBM)- A scientific crystal ball, Pacific Northwest and National Laboratory, Richland, WA, *International Congress on Advanced Nuclear Power Plants*, 194 (2002) 194-1-7.

[10] D. N. Johnston, Numerical modelling of reciprocating pumps with self-acting valves, *Proceedings of the Institution of Mechanical Engineers, Part I: J. of Systems and Control Engineering*, 205 (2) (1991) 87-96.

[11] P. J. Singh and N. K. Madavan, Complete analysis and simulation of reciprocating pumps including system piping, *Proceedings of the Fourth International Pump Symposium* (1987) 55-73.

[12] T. Henshaw, Power pump valve dynamics-a study of the velocity and pressure distribution in outward-flow bevel-face and flat-face power pump valves, *Proceedings of 25th International Conference Pump Users Symposium* (2009) 23-32.

[13] S. D. Able, Reciprocating pump acceleration head, *Proceedings of ASME FEDSM01-2001 ASME Fluids Engineering Division Summer Meeting*, New Orleans (2001) 1-7.

[14] V. E. Shcherba, E. A. Pavlyuchenko and A. K. Kuz-

hbanov, Parametric analysis of operation of pumping section of reciprocating pump compressor with gas damper, *Chemical and Petroleum Engineering,* 50 (1-2) (2014) 33-37.

[15] J. J. Rudolf, T. R. Heidrick, B. A. Fleck and V. S. V. Rajan, Optimum design parameters for reciprocating pumps used in natural gas wells, *J. of Energy Resources Technology,* 127 (4) (2005) 285-292.

[16] F. M. White, *Fluid Mechanics*, McGraw-Hill, New York, USA (1994).

[17] A. G. Erdman and G. N. Sandor, *Mechanism Design*, Prentice Hall, New Jersey, USA (1991).

[18] Y. Cengel and J. Cimbala, *Fluid Mechanics: Fundamentals and Applications*, McGraw-Hill, New York, USA (2013).

[19] D. McCloy and H. R. Martin, *Control of Fluid Power: Analysis and Design*, Ellis Horwood Ltd., New York, USA (1980).

[20] D. An and J. H. Choi, Improved MCMC method for parameter estimation based on marginal probability density function, *JMST,* 27 (6) (2013) 1771-1779.

Jong Kyeom Lee received the B.S. in the Division of Mechanical Engineering from Ajou University in South Korea in 2014. He is currently a combined master's and doctoral program candidate at the Multiscale Noise and Vibration Lab. at Ajou University. His research interests are machine diagno-stics and optimal design by using statistical methods.

Jun Ki Jung received his B.S. in the Division of Mechanical Engineering from Ajou University in South Korea in 2013. He is currently a Master's student at Ajou University. His research interest is machine diagnostics.

Jangbom Chai is a Professor in the Department of Mechanical Engineering at Ajou University. He has the B.S. and the M.S. in Mechanical Engineering from Seoul National University in Korea in 1984 and 1986, respectively. He obtained the Ph.D. in Mechanical Engineering from MIT in 1993. He received the O. Hugo Schuck Best Paper Award from American Automatic Control Council and the awards from Korean Nuclear Society and Korean Society of Pressure Vessel and Piping.

Jin Woo Lee is an Associate Professor of Mechanical Engineering at Ajou University. His research interests are in the area of vibrations, acoustics, topology optimization based design and fluid-structure interactions of microcantielvers for RF-MEMS and AFM. He received the Ph.D. in School of Mechanical and Aerospace Engineering from Seoul National University in South Korea in 2003.